J|A|C|S
COMMUNICATIONS

Published on Web 01/26/2006

Hot Spots in Silver Nanowire Bundles for Surface-Enhanced Raman Spectroscopy

Seung Joon Lee, Andrew R. Morrill, and Martin Moskovits*

Department of Chemistry & Biochemistry, University of California, Santa Barbara, California 93106

Received November 17, 2005; E-mail: mmoskovits@ltsc.ucsb.edu

Surface-enhanced Raman spectroscopy (SERS) was discovered approximately 25 years ago and has been studied diligently ever since. The effect occurs at the surfaces of certain nanostructured materials primarily due to the concentration of electromagnetic (EM) near-fields associated with strong, localized surface plasmon resonances.[1] In addition to EM enhancement, a number of other processes have been postulated and observed to lead to enhancement, such as charge-transfer resonances.[2] Most SERS-enhancing systems consist of several, and often a very large number of, coupled nanoparticles or of nanostructured surfaces consisting of closely spaced features.

Over the past decade, a number of exciting new experimental and theoretical advances have occurred in SERS.[3] It is now largely understood that in a number of systems SERS is a highly heterogeneous process due to local enhancements at certain "hot spots" of the order of $\sim 10^{11}$. Two classes of systems have been predicted to produce such super-hot sites: small nanoparticle dimers and aggregates in which interstitial sites are the super-enhancing locations, and large fractal aggregates in which the hot spots arise from the symmetry breaking that occurs when the fractal cluster that possesses scaling symmetry is excited with an EM field that does not.[4] The weight of experimental evidence points to the fact that it is these hot spots that are responsible for the major part of the giant enhancements ($\sim 10^{14}$) reported by Nie[5] and by Kneipp[6] and later corroborated by the work of Käll[7] and Brus[8]—enhancements high enough to allow almost routine detection of Raman from single molecules.

On the basis of these considerations, a great deal of the current research effort in SERS focuses on the controlled and reproducible fabrication of metallic nanostructures that produce hot geometries where the molecules are appropriately and predictably located for giant Raman enhancement. Recently, several strategies have been proposed for preparing such hot structures for chemical and biological sensing applications. These include probes that incorporate dimer-like nanoaggregates[9] and highly ordered, periodic 2-D nanostructures.[10] Although these efforts illustrate the potential for using SERS as a sensitive molecular sensing tool, there remains room for optimization. Reproducible aggregation of solution-phase nanoparticles is hard to control, and fabricating periodic structures with interparticle gap dimensions $<\sim 2$ nm (necessary for intense SERS enhancement) challenges current nanofabrication technology.

In this connection, we demonstrate a simple strategy for obtaining hot spots of the form "metal/molecule/metal", which automatically positions many analyte molecules in the junction between neighboring tips of Ag nanowires that were fabricated in porous aluminum oxide (PAO) then exposed by the controlled dissolution of the alumina matrix.

Silver nanowires were grown in highly ordered PAO template by AC electrodeposition.[11] To maximize the system's cleanliness and the uniformity of silver filling, the backside (i.e., the barrier-layer side) of the Ag-filled PAO (Ag−PAO) template was the surface at which the experiment was carried out. The aluminum backing was removed, and the alumina matrix was partially etched to expose the tips of nanowires.

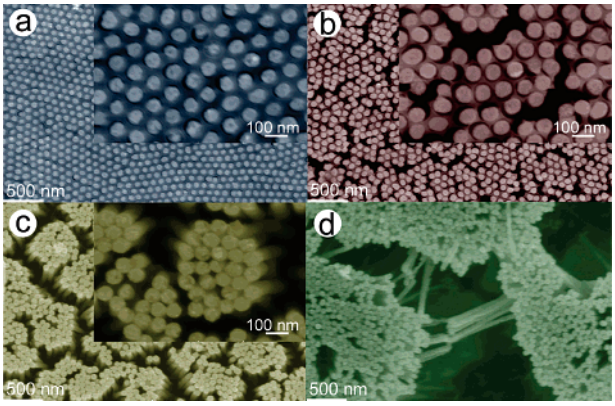

Figure 1. SEM images of BT-modified Ag−PAO templates obtained by partial dissolution of the alumina matrix in 0.1 M aqueous NaOH for (a) 0 s, (b) 210 s, (c) 270 s, and (d) 450 s.

The Raman experiments were performed in two ways using benzenethiol (BT) as a Raman probe. In the "add-analyte-then-etch" version, only the tips of the nanowires are functionalized with BT before the etching process is carried out that allows the silver nanowire tips ultimately to touch. In the "etch-then-add-analyte" protocol, the etching is carried out first, then BT is allowed to functionalize the entire length of the nanowires, so that the SERS signal observed presumably arises primarily from those molecules which find appropriate clefts and interstices as happenstance allows.

First, for the results of the add-analyte-then-etch experiment, Figure 1a shows the SEM image of BT-exposed Ag−PAO before the etching process was carried out. The tips of Ag nanowires protrude slightly above the oxide matrix. At this point, the SERS signal is very weak (Figure 2Ba). SEM images of (BT-covered) Ag nanowire tips are shown as a function of etching time in aqueous 0.1 M NaOH in b−d of Figure 1. The corresponding intensity of the 1573 cm^{-1} SERS band as a function of etch time as well as representative SERS spectra is also displayed in Figure 2. At the early stages of the etching process (up to $\sim$210 s), pore-widening of the PAO template is observed accompanied by a slight increase in the protrusion of the Ag nanowires above the alumina matrix (Figure 1b). At this stage, the gap between tips of neighboring nanowires is approximately $<$20 nm, implying that the EM gap field is still rather weak, and indeed, at the beginning of the etching process, an almost unchanging and weak SERS signal is observed, so long as the silver nanowires are unable to bend sufficiently so as to reduce the inter-nanowire gap size (Figure 2Ba).

After $\sim$270 s of etching, a sufficient length of the nanowire is freed from its matrix to allow the tips of the nanowires to bend toward each other (possibly due to van der Waals attraction between the nanowires), forming closely interacting bundles, thereby trapping

10.1021/ja0578350 CCC: $33.50

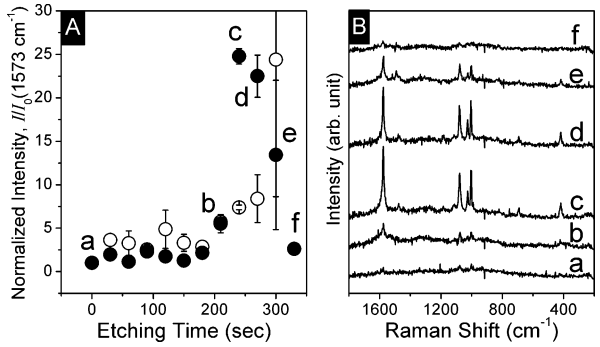

Figure 2. (A) Normalized intensities of the 1573 cm^{-1} band plotted as a function of the etching time at 30 s intervals; filled circles correspond to the add-analyte-then-etch experiment, and the open circles to the etch-then-add-analyte experiment. (B) Selected SERS spectra, obtained in the add-analyte-then-etch experiment, corresponding to the various etching times indicated in A.

and automatically positioning analyte molecules pre-adsorbed at the tips of the nanowires in the junctions between neighboring tips. Recalling the aforementioned fact that electromagnetic hot spots tend to be gap modes in the interstice between closely spaced metallic nanostructures,[3] intense EM field enhancement is expected for this tip/analyte/tip arrangement. The SERS spectra, in fact, show a significant (∼25-fold) intensity increase over its initial value at this point (Figure 2Bc and 2Bd). As the etching progresses to ∼450 s, the sizes of bundles continue to grow, but the SERS intensity decreases and eventually disappears (Figure 2Be and 2Bf). This abrupt decrease in SERS intensity might be due to the reduction in the integrity of the tip-to-tip geometry when the last of the alumina matrix is etched away, reducing the stability of the nanowire bundles, which will now have lost their anchor in the alumina template (Figure 1d). We estimate that on average ∼80 nanowires are illuminated by our laser. Assuming that on each nanowire the analyte covers a hemispherical cap with ∼35 nm radius, we estimate that at most $\sim 3.3 \times 10^{-18}$ mol (i.e., $\sim 2.0 \times 10^{6}$ molecules) are being sampled by the laser in the add-analyte-then-etch experiments. This estimate is a lower bound for the following reasons: the nanowires are unlikely to be fully covered with adsorbate, a larger than diffraction-limited laser spot size was assumed, and only a fraction of the adsorbed molecules occupy gap sites between the almost-touching nanowire tips.

For the etch-then-add-analyte experiments, the SEM images were much the same as those shown in Figure 1 after etching for equivalent lengths of time. The dependence of the SERS intensities on etching time differs, however, from what was observed in the former set (Figure 2A, open circles). Even after ∼240 s of etching, the SERS intensities remain weak and only reach the intensity levels of the add-analyte-then-etch experiment after ∼300 s of etching. Moreover, the SERS intensity does not decrease on further etching but reaches a saturation value after ∼450 s of etching, at which point the SERS intensity is ∼50-fold the initial value (i.e., the value observed after only moderate etching). At this point, the maximum SERS intensity achieved in the two experiments is approximately equal (within a factor of 2), even though in the former set only the tips of the nanowires were coated with analyte, while in the latter, the entire length of the nanowire (∼5 μm) is covered with analyte, implying that the average enhancement achieved in the add-analyte-then-etch approach exceeds that in the etch-first approach by at least a factor of $\sim 1.3 \times 10^{2}$. This behavior is easily understood. In the add-analyte-then-etch approach, many analyte molecules will be positioned within the gaps created by the collapsing nanowire tips and, therefore, benefit from the giant electromagnetic fields that exist in those hot spots. While in the etch-then-add-analyte approach, the molecules adsorb along the entire lengths of the nanowires and only occasionally find themselves in hot clefts and gaps that happen to have formed. Moreover, the availability of gaps might be reduced by the fact that without the molecular species pre-adsorbed on the nanowires most nanowires will touch upon their collapse, making the gap inaccessible to the analyte.

In summary, we report a simple strategy for placing analyte molecules in hot spots between closely spaced nanowires leading to intense SERS enhancement. The results are highly reproducible from experiment to experiment likely because of the regularity of the SERS substrate, which consists of highly ordered and regular silver nanowires fabricated in porous aluminum oxide. Because the silver nanowires are sealed in the pores of PAO, this system is potentially immune to contamination until it is ready for use, at which point the alumina matrix is etched, thereby allowing the silver nanowires to collapse into bundles and form hot spots in the region of close contact between the nanowires, trapping the analyte in those junctions.

Acknowledgment. Funding from the Institute for Collaborative Biotechnologies through Grant DAAD19-03-D- 0004 from the U.S. Army Research Office and from Lawrence Livermore National Laboratories through a UCDRD grant is gratefully acknowledged. Helpful discussions with Martin Schierhorn and Dr. Ioana Pavel are gratefully acknowledged.

Supporting Information Available: The experimental details and two helpful figures are available. This material is available free of charge via the Internet at http://pubs.acs.org.

References

(1) Moskovits, M. *Rev. Mod. Phys.* **1985**, *57*, 783−826.
(2) Otto, A.; Mrozek, I.; Grabhorn, H.; Akemann, W. *J. Phys.: Condens. Matter* **1992**, *4*, 1143−1212.
(3) (a)Futamata, M.; Maruyama, Y.; Ishikawa, M. *J. Phys. Chem. B* **2003**, *107*, 7607−7617. (b) Drachev, V. P.; Perminov, S. V.; Rautian, S. G.; Safonov, V. P. *Top. Appl. Phys.* **2002**, *82*, 113−147. (c) Xu, H.; Aizpurua, J.; Käll, M.; Apell, P. *Phys. Rev. E* **2000**, *62*, 4318−4324. (d) Markel, V. A.; Shalaev, V. M.; Zhang, P.; Huynh, W.; Tay, L.; Haslett, T. L.; Moskovits, M. *Phys. Rev. B* **1999**, *59*, 10903−10909. (e) García-Vidal, F. J.; Pendry, J. B. *Phys. Rev. Lett.* **1996**, *77*, 1163−1166.
(4) (a) Gresillon, S.; Aigouy, L.; Boccara, A. C.; Rivoal, J. C.; Quelin, X.; Desmarest, C.; Gadenne, P.; Shubin, V. A.; Sarychev, A. K.; Shalaev, V. M. *Phys. Rev. Lett.* **1999**, *82*, 4520−4523. (b) Shalaev, V. M.; Sarychev, A. K. *Phys. Rev. B* **1998**, *57*, 13265−13288. (c) Stockman, M. I. *Phys. Rev. E* **1997**, *56*, 6494−6507. (d) Shalaev, V. M.; Botet, R.; Mercer, J.; Stechel, E. B. *Phys. Rev. B* **1996**, *54*, 8235−8242.
(5) (a) Krug, J. T.; Wang, G. D.; Emory, S. R.; Nie, S. *J. Am. Chem. Soc.* **1999**, *121*, 9208−9214. (b) Emory, S. R.; Haskins, S.; Nie, S. *J. Am. Chem. Soc.* **1998**, *120*, 8009−8010. (c) Nie, S.; Emory, S. R. *Science* **1997**, *275*, 1102−1106.
(6) (a) Kneipp, K.; Kneipp, H.; Kartha, V. B.; Manoharan, R.; Deinum, G.; Itzkan, I.; Dasari, R. R.; Feld, M. S. *Phys. Rev. E* **1998**, *57*, R6281−R6284. (b) Kneipp, K.; Wang, Y.; Kneipp, H.; Perelman, L. T.; Itzkan, I.; Dasari, R. R.; Feld, M. S. *Phys. Rev. Lett.* **1997**, *78*, 1667−1670. (c) Kneipp, K.; Wang, Y.; Kneipp, H.; Itzkan, I.; Dasari, R. R.; Feld, M. S. *Phys. Rev. Lett.* **1996**, *76*, 2444−2447.
(7) (a) Eliasson, C.; Loren, A.; Murty, K. V. G. K.; Josefson, M.; Käll, M.; Abrahamsson, J.; Abrahamsson, K. *Spectrochim. Acta A* **2001**, *57*, 1907−1915. (b) Xu, H.; Bjerneld, E. J.; Käll, M.; Borjesson, L. *Phys. Rev. Lett.* **1999**, *83*, 4357−4360. (c) Gunnarsson, L.; Petronis, S.; Kasemo, B.; Xu, H.; Bjerneld, J.; Käll, M. *Nanostruct. Mater.* **1999**, *12*, 783−788.
(8) (a) Bosnick, K. A.; Jiang, J.; Brus, L. *J. Phys. Chem. B* **2002**, *106*, 8096−8099. (b) Michaels, A. M.; Jiang, J.; Brus, L. *J. Phys. Chem. B* **2000**, *104*, 11965−11971.
(9) Su, X.; Zhang, J.; Sun, L.; Koo, T.-W.; Chan, S.; Sundararajan, N.; Yamakawa, M.; Berlin, A. A. *Nano Lett.* **2005**, *5*, 49−54.
(10) Stuart, D. A.; Yonzon, C. R.; Zhang, X.; Lyandres, O.; Shah, N. C.; Glucksberg, M. R.; Walsh, J. T.; Van Duyne, R. P. *Anal. Chem.* **2005**, *77*, 4013−4019.
(11) (a) Al-Mawlawi, D.; Liu, C. Z.; Moskovits, M. *J. Mater. Res.* **1994**, *9*, 1014−1018. (b) Masuda, H.; Fukuda, K. *Science* **1995**, *268*, 1466−1468.

JA0578350